IEEE Photonics Journal
An IEEE Photonics Society Publication

Open Access

All-Optical OFDM Generation for IEEE802.11a Based on Soliton Carriers Using Microring Resonators

Volume 6, Number 1, February 2014

S. E. Alavi
I. S. Amiri
S. M. Idrus
A. S. M. Supa'at
J. Ali
P. P. Yupapin

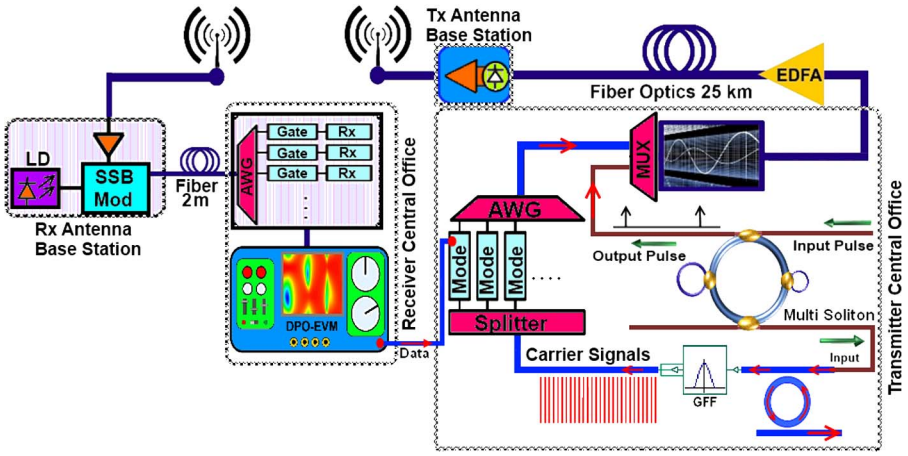

DOI: 10.1109/JPHOT.2014.2302791
1943-0655 © 2014 IEEE

IEEE photonics SOCIETY

IEEE

All-Optical OFDM Generation for IEEE802.11a Based on Soliton Carriers Using Microring Resonators

S. E. Alavi,[1] I. S. Amiri,[2] S. M. Idrus,[1] A. S. M. Supa'at,[1] J. Ali,[2] and P. P. Yupapin[3]

[1]Lightwave Communication Research Group, Faculty of Electrical Engineering, Universiti Teknologi Malaysia (UTM), 81310 UTM Skudai, Johor, Malaysia
[2]Institute of Advanced Photonics Science, Nanotechnology Research Alliance, Universiti Teknologi Malaysia (UTM), 81310 Johor Bahru, Malaysia
[3]Advanced Research Center for Photonics, Department of Applied Physics, Faculty of Science, King Mongkut's Institute of Technology Ladkrabang, Bangkok 10520, Thailand

DOI: 10.1109/JPHOT.2014.2302791

Manuscript received January 5, 2014; revised January 22, 2014; accepted January 22, 2014. Date of publication January 27, 2014; date of current version February 5, 2014. This work was supported by the Ministry of Science, Technology and Innovation, Malaysia, through eScience funding under Project 06-01-06-SF1148. Corresponding author: S. M. Idrus (e-mail: sevia@fke.utm.my).

Abstract: The optical carrier generation is the basic building block to implement all-optical orthogonal frequency-division multiplexing (OFDM) transmission. One method to optically generate single and multicarriers is to use the microring resonator (MRR). The MRRs can be used as filter devices, where generation of high-frequency (GHz) soliton signals as single and multicarriers can be performed using suitable system parameters. Here, the optical soliton in a nonlinear fiber MRR system is analyzed, using a modified add/drop system known as a Panda ring resonator connected to an add/drop system. In order to set up a transmission system, i.e., IEEE802.11a, first, 64 uniform optical carriers were generated and separated by a splitter and modulated; afterward, the spectra of the modulated optical subcarriers are overlapped, which results one optical OFDM channel band. The quadrature amplitude modulation (QAM) and 16-QAM are used for modulating the subcarriers. The generated OFDM signal is multiplexed with a single-carrier soliton and transmitted through the single-mode fiber (SMF). After photodetection, the radio frequency (RF) signal was propagated. On the receiver side, the RF signal was optically modulated and processed. The results show the generation of 64 multicarriers evenly spaced in the range from 54.09 to 55.01 GHz, where demodulation of these signals is performed, and the performance of the system is analyzed.

Index Terms: Panda ring resonator, soliton carriers, IEEE802.11a, OFDM.

1. Introduction

In this new era of wireless and wired communication systems, orthogonal frequency-division multiplexing (OFDM) [1]–[3] has gained considerable attention to be used as a modulation technology, and it is recognized as a main building block of communications standards such as IEEE 802.11a/g. In OFDM, data are transmitted through many subcarriers, which are orthogonal to each other. Channel equalization is provided in the frequency-domain with a relatively simple solution than conventional time-domain equalization [4]. Besides high spectral efficiency, OFDM has high tolerance to multi-path interference, channel dispersion, and frequency-selective fading.

Moreover, because of the dynamic bandwidth allocation and adaptive bit rate functionalities, the OFDM system has a prominent flexibility [5]. During the last decade, network traffic has increased drastically [6]. To satisfy the demand for new large bandwidth applications, many different methods have been proposed to improve the capacity and efficiency based on the optical transmission of signals. OFDM is also used in optical communication, and it has the superior robustness to fiber chromatic dispersion and polarization mode dispersion (PMD) [7], [8].

An OFDM system includes a inverse fast Fourier transform (IFFT) block at the transmitter and a fast Fourier transform (FFT) block at the receiver. These blocks are usually implemented in the electrical domain enabled by high-speed digital-signal-processing (DSP) devices, but these devices are challenging both commercially and technically. In this regard, all-optical techniques are becoming of interest and are being investigated to reduce the challenges of the electrical domain. These techniques are based on the optically generated and processed OFDM signals using passive optical devices [9], [10]. Transmission of all-optical OFDM is implemented first by generating the multiple optical subcarriers, then separating by optical devices, and finally modulating each subcarrier independently [11], [12]. Therefore, an optical carrier generation is the basic building block to implement the OFDM transmission fully in the optical domain.

One method to generate the multi-carriers optically is to use a microring resonator (MRR) [13], [14]. Nonlinear light behavior inside an MRR occurs when a strong pulse of light is inputted into the ring system [15]–[17]. The properties of a ring system can be modified via various control methods [16]. MRRs can be used as filter devices where generation of high frequency (GHz) soliton signals can be performed using suitable system parameters [18]. The modified add/drop system known as a Panda ring resonator system consists of a centered ring resonator connected to two smaller MRRs on the right and left sides and is used in many applications in optical communication and signal processing [19]–[21]. This system can be used to generate optical soliton pulses of GHz frequency, thus providing required signals used in a wired/wireless optical communication, such as all optical OFDM, to be applied for IEEE standards, i.e., 802.11a.

In this study, a Panda ring resonator connected to an add/drop system is used to generate non-uniform carrier signals. The uniform shape of these signals can be obtained using the gain flattening filter (GFF) system [22], [23]. The uniform carrier signals are then applied to implement the optical OFDM suitable for the IEEE802.11a standard communication systems. The experimental results show that MRR systems support both the single- and multicarrier optical soliton pulses that are used in an OFDM transmitter/receiver system. Here, the optical soliton in a nonlinear fiber MRR system is analyzed, in order to generate a high frequency band of pulses as single and multi-carriers. The multi-carriers are separated by a splitter and then modulated. The spectra of the modulated optical subcarriers obtained are overlapped, resulting in one optical OFDM channel band. The generated OFDM signal is multiplexed with a single carrier soliton and transmitted through the single mode fiber (SMF). After being beaten to the photodiode, an IEEE802.11a signal is propagated wirelessly in the transmitter antenna base station and received by the second antenna. The bit error rate (BER) and overall system performance are discussed.

2. Theoretical Background

The system of GHz frequency band generation is shown in Fig. 1. Here, a Panda ring resonator is used. The filtering process of the input soliton pulses is performed via the system. The frequency band ranges from 46 to 58 GHz can be obtained.

The two MRRs embedded in the Panda ring resonator have Kerr effect-type nonlinearity. The Kerr effect causes the refractive index (n) of the medium to vary and is given by

$$n = n_0 + n_2 I = n_0 + \frac{n_2}{A_{\text{eff}}} P \tag{1}$$

where n_0 and n_2 are the linear and nonlinear refractive indexes, respectively [24]. Here, I and P are the optical intensity and the power, respectively [25]. The effective mode core area given by

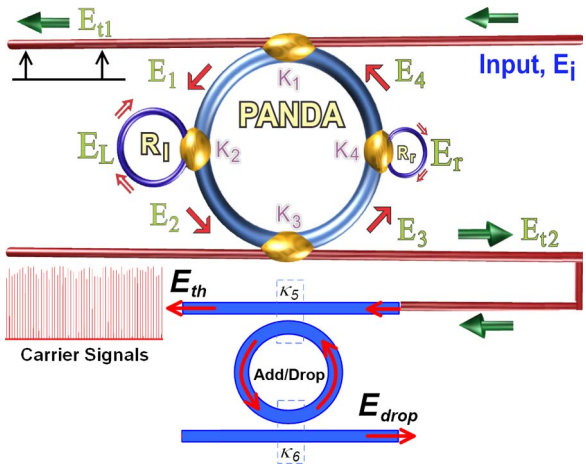

Fig. 1. Optical frequency band generation system using a Panda ring resonator connected to an add/drop system.

A_{eff} ranges from 0.10 to 0.25 μm^2, in terms of practical material parameters (InGaAsP/InP) [26]. A bright soliton with a central frequency of 51 GHz and power of 1 W is introduced into the Panda ring resonator, which is expressed by E_i. The input optical field of the bright soliton is given by [27]

$$E_i = A\text{sech}\left[\frac{T}{T_0}\right]\exp\left[\left(\frac{z}{2L_D}\right) - i\omega_0 t\right] \tag{2}$$

where A and z are the amplitude of optical field and the propagation distance, respectively [28]; L_D is the dispersion length of the soliton pulse; and the carrier frequency of the signal is ω_0 [29]. The soliton pulse keeps its temporal width invariance while it propagates. A balance should be achieved between the dispersion length (L_D) and the nonlinear length $(L_{\text{NL}} = 1/\Gamma\phi_{\text{NL}})$ [30], [31]. Here, $\Gamma = n_2 \times k_0$ is the length scale over which dispersion or nonlinear effects make the beam become wider or narrower. Hence, $L_D = L_{\text{NL}}$ [32]. After the bright soliton is fed into the Panda ring resonator, it round-trips within the two MRRs embedded in the system; therefore, with respect to the Kerr effect nonlinear condition of the rings, the resonant outputs are formed. Thus, the normalized output of the light field is defined as the ratio between the output and input fields [$E_{\text{out}}(t)$ and $E_{\text{in}}(t)$] in each round-trip. This is given for the left and right MRRs as follows:

$$\left|\frac{E_{\text{out}}(t)}{E_{\text{in}}(t)}\right|^2 = (1-\gamma_2)\left[1 - \frac{\left(1-(1-\gamma_2)x_2^2\right)\kappa_2}{\left(1-x_2\sqrt{1-\gamma_2}\sqrt{1-\kappa_2}\right)^2 + 4x_2\sqrt{1-\gamma_2}\sqrt{1-\kappa_2}\sin^2\left(\frac{\phi_2}{2}\right)}\right] \tag{3}$$

$$\left|\frac{E_{\text{out}}(t)}{E_{\text{in}}(t)}\right|^2 = (1-\gamma_4)\left[1 - \frac{\left(1-(1-\gamma_4)x_4^2\right)\kappa_4}{\left(1-x_4\sqrt{1-\gamma_4}\sqrt{1-\kappa_4}\right)^2 + 4x_4\sqrt{1-\gamma_4}\sqrt{1-\kappa_4}\sin^2\left(\frac{\phi_4}{2}\right)}\right]. \tag{4}$$

This equation indicates that an MRR, in this particular case, is very similar to a Fabry–Perot cavity, which has an input and an output mirror with a field reflectivity, $(1-\kappa)$, and a fully reflecting mirror. κ is the coupling coefficient, γ is the fractional coupler intensity loss, $x = \exp(-\alpha L/2)$ represents a round-trip loss coefficient, $\phi = \phi_0 + \phi_{\text{NL}}$, $\phi_0 = kLn_0$ and $\phi_{\text{NL}} = kLn_2|E_{\text{in}}|^2$ are the linear and nonlinear phase shifts, and $k = 2\pi/\lambda$ is the wave propagation number in a vacuum. L and α are the waveguide length and linear absorption coefficient, respectively. In this work, the iterative method is introduced to obtain the resonant results and, similarly, when the output field is connected and input

into the other MRRs [33], [34]. In the case of the add/drop system, the nonlinear refractive index is neglected [35]–[37]. The obtained signals are given as follows [38]:

$$E_1 = \sqrt{1-\gamma_1}(\sqrt{1-\kappa_1}E_4 + j\sqrt{\kappa_1}E_i) \tag{5}$$

$$E_2 = E_L E_1 e^{-\frac{\alpha L}{22} - jk_n\frac{L}{2}} \tag{6}$$

$$E_3 = \sqrt{1-\gamma_3} \times \sqrt{1-\kappa_3}E_2 \tag{7}$$

$$E_4 = E_r E_3 e^{-\frac{\alpha L}{22} - jk_n\frac{L}{2}} \tag{8}$$

where $L = 2\pi R_{\text{Panda}}$, and R_{Panda} is the radius of the Panda ring resonator. The E_L and E_r are given by [39]

$$E_L = E_1 \frac{\sqrt{(1-\gamma_2)(1-\kappa_2)} - (1-\gamma_2)e^{-\frac{\alpha}{2}L_L - jk_nL_L}}{1-\sqrt{1-\gamma_2}\sqrt{1-\kappa_2}e^{-\frac{\alpha}{2}L_L - jk_nL_L}} \tag{9}$$

$$E_r = E_3 \frac{\sqrt{(1-\gamma_4)(1-\kappa_4)} - (1-\gamma_4)e^{-\frac{\alpha}{2}L_R - jk_nL_R}}{1-\sqrt{1-\gamma_4}\sqrt{1-\kappa_4}e^{-\frac{\alpha}{2}L_R - jk_nL_R}} \tag{10}$$

where $L_R = 2\pi R_r$, $R_r = 8\ \mu$m, $L_L = 2\pi R_l$, $R_l = 18\ \mu$m. Therefore, the output signals from the through and drop ports of the Panda ring resonator can be expressed as [40], [41]

$$E_{t1} = \sqrt{1-\gamma_1}[\sqrt{1-\kappa_1}E_i + j\sqrt{\kappa_1}E_4] \tag{11}$$

$$E_{t2} = \sqrt{1-\gamma_3} \times j\sqrt{\kappa_3}E_2. \tag{12}$$

In order to generate multi-carriers, the output from the Panda ring resonator is fed into the add/drop system shown in Fig. 1. Therefore, to retrieve the signals from the chaotic signals, we propose to use the add/drop system with the appropriate parameters. The transmitted output can be controlled and obtained by choosing suitable key parameters such as the coupling ratio of the system [42]. The two output electric fields of the add/drop system can be expressed by E_{th} and E_{drop} [43], as follows:

$$\begin{aligned}\frac{E_{\text{th}}}{E_{t2}} &= \frac{-\kappa_5\sqrt{1-\kappa_6}e^{\frac{-\alpha}{2}L_{\text{ad}} - jk_nL_{\text{ad}}} + \sqrt{1-\kappa_5} - (1-\kappa_5)\sqrt{1-\kappa_6}e^{\frac{-\alpha}{2}L_{\text{ad}} - jk_nL_{\text{ad}}}}{1-\sqrt{1-\kappa_5}\sqrt{1-\kappa_6}e^{\frac{-\alpha}{2}L_{\text{ad}} - jk_nL_{\text{ad}}}} \\ &= \frac{-\sqrt{1-\kappa_6}e^{\frac{-\alpha}{2}L_{\text{ad}} - jk_nL_{\text{ad}}} + \sqrt{1-\kappa_5}}{1-\sqrt{1-\kappa_5}\sqrt{1-\kappa_6}e^{\frac{-\alpha}{2}L_{\text{ad}} - jk_nL_{\text{ad}}}}\end{aligned} \tag{13}$$

$$\begin{aligned}\frac{E_{\text{drop}}}{E_{t2}} &= \frac{j\sqrt{\kappa_5}}{1-\sqrt{1-\kappa_5}\sqrt{1-\kappa_6}e^{\frac{-\alpha}{2}L_{\text{ad}} - jk_nL_{\text{ad}}}} e^{\frac{-\alpha}{4}L_{\text{ad}} - jk_n\frac{L_{\text{ad}}}{2}} j\sqrt{\kappa_6} \\ &= \frac{-\sqrt{\kappa_5\cdot\kappa_6}e^{\frac{-\alpha}{4}L_{\text{ad}} - jk_n\frac{L_{\text{ad}}}{2}}}{1-\sqrt{1-\kappa_5}\sqrt{1-\kappa_6}e^{\frac{-\alpha}{2}L_{\text{ad}} - jk_nL_{\text{ad}}}}.\end{aligned} \tag{14}$$

The normalized intensity powers of the through and drop ports are then obtained as follows [44]:

$$\left|\frac{E_{\text{th}}}{E_{t2}}\right|^2 = \frac{1-\kappa_5 - 2\sqrt{1-\kappa_5}\sqrt{1-\kappa_6}e^{\frac{-\alpha}{2}L_{\text{ad}}}\cos(k_nL_{\text{ad}}) + (1-\kappa_6)e^{-\alpha L_{\text{ad}}}}{1+(1-\kappa_5)(1-\kappa_6)e^{-\alpha L_{\text{ad}}} - 2\sqrt{1-\kappa_5}\sqrt{1-\kappa_6}e^{\frac{-\alpha}{2}L_{\text{ad}}}\cos(k_nL_{\text{ad}})} \tag{15}$$

$$\left|\frac{E_{\text{drop}}}{E_{t2}}\right|^2 = \frac{\kappa_5\cdot\kappa_6 e^{\frac{-\alpha}{2}L_{\text{ad}}}}{1+(1-\kappa_5)(1-\kappa_6)e^{-\alpha L_{\text{ad}}} - 2\sqrt{1-\kappa_5}\sqrt{1-\kappa_6}e^{\frac{-\alpha}{2}L_{\text{ad}}}\cos(k_nL_{\text{ad}})}. \tag{16}$$

Here, L_{ad} is the add/drop system length, where $L_{\text{ad}} = 2\pi R_{\text{ad}}$, and κ_5 and κ_6 are the coupling coefficients.

TABLE 1

Fixed and variable parameters of the MRR system

Fixed Parameters	R_{Panda}	R_{ad}	R_1	R_r	κ_1	κ_2	κ_3	κ_4	κ_5
	100μm	20μm	18μm	8μm	0.35	0.22	0.3	0.1	0.1
	κ_6	n_0	n_2 (m^2W^{-1})	A_{eff1} (μm²)	A_{eff3} (μm²)	A_{effL} (μm²)	A_{effR} (μm²)	α ($dBmm^{-1}$)	γ
	0.3	3.34	2.2×10^{-17}	0.25	0.25	0.12	0.1	0.5	0.1

Variable Parameters	T_0	T	z	L_D	L_{NL}	Φ_{NL}	A	I
	Initial propagation time	Propagation time	Propagation distance	Dispersion length	Nonlinear length	Nonlinear phase shift	Optical amplitude	Optical intensity
	E_1-E_4	E_R	E_L	E_{t1}	E_{t2}	E_{th}	E_{drop}	P
	electric fields	Electric field of the right ring	Electric field of the left ring	Throughput electric field	Drop port electric field	Throughput add/drop field	Drop port add/drop field	Optical power

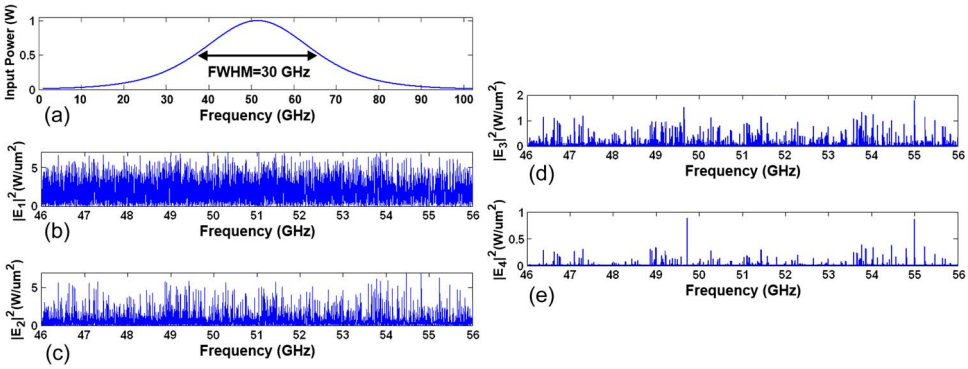

Fig. 2. (a) Input bright soliton, intensities within the system. (b) $|E_1|^2$ (W/μm^2). (c) $|E_2|^2$ (W/μm^2). (d) $|E_3|^2$ (W/μm^2). (e) $|E_4|^2$ (W/μm^2).

3. Experimental Results and Discussion

The fixed and variable parameters of the system are listed in Table 1.

The results of the chaotic signal generation are shown in Fig. 2. The input pulse of a bright soliton with a power of 1 W is fed into the system. This pulse has a bandwidth of 30 GHz and central frequency of 51 GHz shown in Fig. 2(a). Large bandwidth within the system can be generated by using a soliton pulse input into the nonlinear MRRs. The signal is chopped into smaller signals spreading over the spectrum. The soliton signals inside the Panda ring resonator are shown in Fig. 2. Here, the results shown in Fig. 2(b)–(e) are obtained using the square form of the equations (5)–(8), respectively. The filtering and trapping processes occur during propagation of the input soliton pulse inside the two MRRs. Fig. 2(b) and (c) shows the generated signals on the left side of the Panda ring resonator, and Fig. 2(d) and (e) shows the intensities on the right side.

The output signals from the throughput and drop ports of the Panda ring resonator can be seen in Fig. 3(a) and (b). These results are obtained using the square form of the Equations (11) and (12) respectively. Here, the single and multi-solitons frequency ranges from 46 to 58 GHz are generated in wireless local area networks (WLANs) usage. The throughput output (E_{t1}) shows the localized ultra-short soliton pulses with FWHM of 5 MHz and FSR of 5.2 GHz. The soliton pulses at the frequencies of 49.8 and 55 GHz are generated. The drop port output intensity expressed by $|E_{t2}|^2$ is shown in Fig. 3(b). Here, the multi-solitons with FWHM of 20 MHz and FSR of 4 GHz are generated, respectively and fed into the add/drop system. Fig. 3(c) shows the generated multi-carriers from the throughput port of the add/drop system, in which equation (15) is used to obtain this result. The Fig. 3(d) shows the uniform carrier signals using the GFF system.

By using the appropriate parameters, as presented in Table 1, relating to the practical device, such as MRR radii, coupling coefficients, linear and nonlinear refractive indexes, the multi-carriers from the add/drop system can be obtained non-uniformly and finally converted to uniform carrier signals using the GFF system.

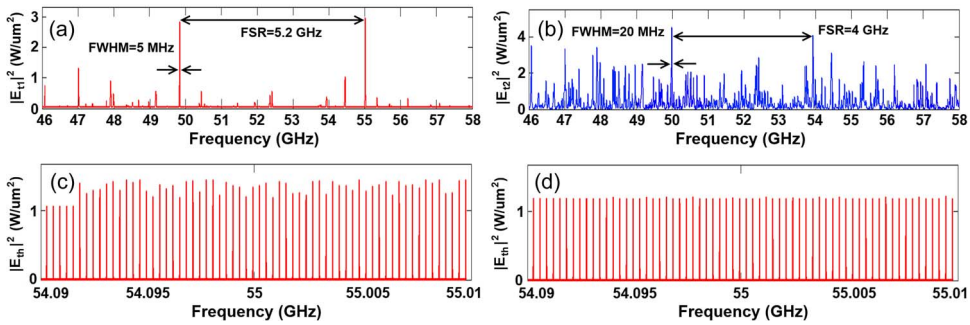

Fig. 3. (a) Throughput output signal with FWHM = 5 MHz and FSR = 5.2 GHz. (b) Multi-soliton range from 46 to 58 GHz with FWHM = 20 MHz and FSR = 4 GHz. (c) Non-uniform multi-carrier generation using the add/drop system. (d) Uniform multi-carrier generation using the GFF system.

Assuming OFDM signaling, the transmitted signal to optical channel is as follows:

$$s(t) = \sum_{m=0}^{M-1} \sum_{i=-\infty}^{\infty} d_m(i) \exp(j2\pi f_m(t - iT_s)) p(t - iT_s) \tag{17}$$

where $d_m(i) = a_m(i) + jb_m(i)$ is the symbol of the mth sub-channel at time interval $[iT_s, (i+1)T_s]$, i.e., for QAM modulation, it is $\pm 1 \pm j$. $p(t)$ is the response of the transmitter filter, which is a rectangular pulse with duration T_s and amplitude 1. Hence

$$p(t) = \begin{cases} 1, & -T_g \le t \le T \\ 0, & \text{otherwise.} \end{cases} \tag{18}$$

T_g is the guard interval of the OFDM signal, T_s is the time difference between the symbol duration, and the guard interval T_g is the effective symbol duration time $T = T_s - T_g$. The frequency of the mth subcarrier should satisfy the orthogonality condition. Hence

$$f_m = f_0 + \frac{m}{T}, \quad m = 0, 1, 2, \ldots, M-1. \tag{19}$$

As for IEEE802.11a, the occupied bandwidth of the channel is 20 MHz. The numbers of the subcarriers are 64, in which 52 of them are modulated. To avoid intersymbol interference (ISI) and intercarrier interference (ICI), $T_g = 0.8$ ms was used. Then, the OFDM symbol interval $T_S = 3.2$ μs, and the subcarrier spacing is $SC_{\text{Spacing}} = (1/T_s) = (1/3.2\ \mu\text{s}) = 312.5$ kHz.

Therefore, the system is designed with $N = 64$ subcarriers. In this system, in order to modulate the subcarriers, QAM and 16-QAM are considered. The schematic of the system setup is shown in Fig. 4. At the transmitter central office (TCO), a Panda ring resonator is connected to an add/drop system, in order to generate 64 multi-carriers evenly spaced in the range of 54.09 to 55.01 GHz, as shown in Fig. 3(d). A single carrier signal is also generated and located at 49.8 GHz, which is illustrated in Fig. 3(a). The distance between the single subcarrier and the center of the multi-carriers is 5.2 GHz, which is the radio frequency (RF) band for IEEE802.11a standard. Multi-carriers are separated by a splitter and are modulated with the data. In order to imitate the IFFT block at the transmitter and FFT at the receiver, an array waveguide grating (AWG) is used. The spectra of the modulated optical subcarriers are overlapped, resulting in one optical OFDM channel band shown in Fig. 5(a).

The generated OFDM signal is multiplexed with a single carrier, and after amplification by an erbium doped fiber amplifier (EDFA), the multiplexed signal is transmitted through the SMF. The fiber optic has a length of 25 km, an attenuation of 0.2 dB/km, dispersion of 5 ps/nm/km, the

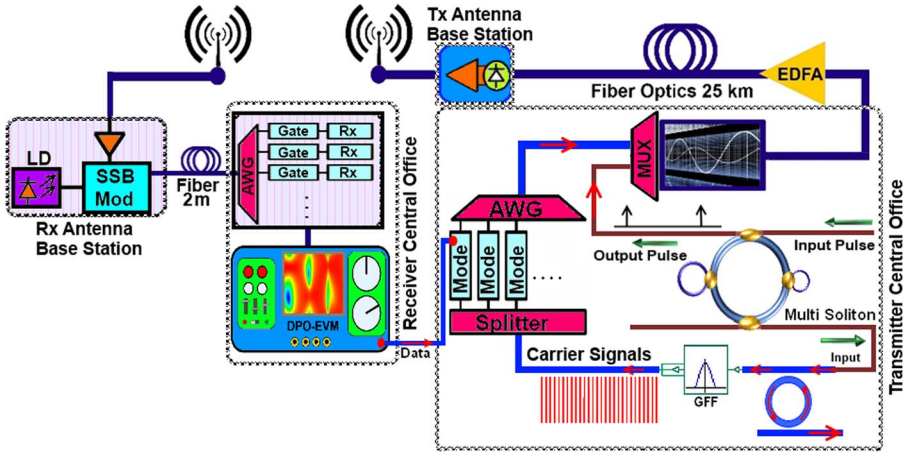

Fig. 4. Experimental system setup.

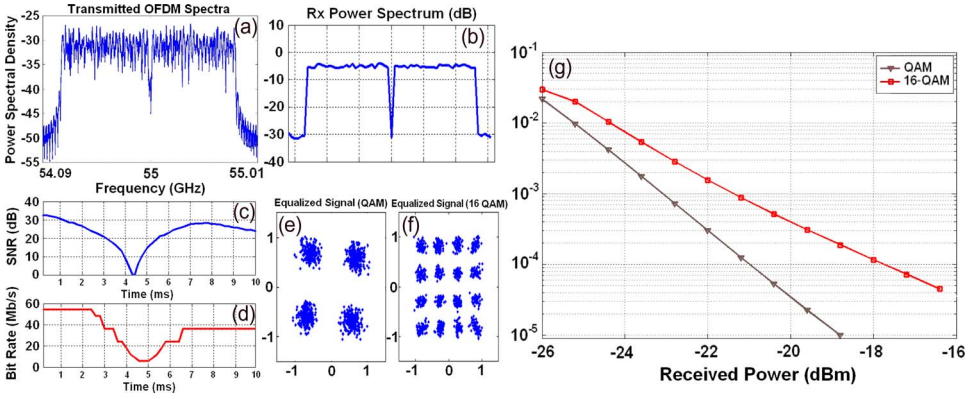

Fig. 5. (a)–(f) Transmitter and receiver performances. (g) QAM and 16-QAM performances.

differential group delay of 0.2 ps/km, the nonlinear refractive index of 2.6×10^{-20} m^2/W, effective area of 25 μm^2, and the nonlinear phase shift of 3 mrad. At the transmitter antenna base station, the multiplexed signals are being beaten to the photodiode. Hence, an IEEE802.11a signal is generated and propagated wirelessly by transmitter antenna and captured by the second antenna located in the receiver, as shown in Fig. 5(b). At the receiver antenna base station, the RF signal is up-converted using a commercially available distributed feedback (DFB) laser to process the received signal optically. The up-converted signal is transmitted to the receiver central office (RCO) through 2m SMF. At the RCO, the AWG is used to implement the FFT function optically. The demodulation is performed, and the BER is calculated. As shown in Fig. 5(c) and (d), the data rate of 56 Mb/s at signal to noise ratio (SNR) of 30 dB is achievable, which implies that the proposed system can be replaced by traditional IEEE802.11a systems. In addition, it shows the bit rate relation to the SNR, where for the SNRs less than 23 dB, the bit rate is getting decreased gradually, and for SNR above 23 dB, the bit rate is constant. Moreover, the constellation diagrams after equalization for QAM and 16-QAM modulated signals are shown in Fig. 5(e) and (f) respectively, which shows a good performance of both scenarios. A further investigation on the system performance is conducted using a BER calculation. As illustrated in Fig. 5(g), the system performance under two circumstances is investigated, which are QAM and 16-QAM modulations. This figure implies that higher received power corresponds to better performance of the QAM modulation than 16-QAM.

Based on the presented system and results, it is possible to use the MRR to generate both single and multi-carriers to be applied for optical OFDM signal generation. IEEE802.11a is a common application that can be benefited from this system.

4. Conclusion

A Panda ring resonator connected to an add/drop system has been demonstrated. An optical soliton frequency band is generated by the input bright soliton pulse propagating within the system. A high frequency band of optical soliton pulses can be generated and used in optical communication networks such as IEEE802.11a, for single and multi-carriers. Thus, high bit rate data transmission using broad soliton frequency band can be provided. An all optical OFDM signal was generated based on the multi-carriers from MRRs via a wired/wireless communication network. The system performance was investigated for QAM and 16-QAM modulations. Hence, the higher received power corresponds to better performance of QAM than 16-QAM modulation. Therefore, the multi-carriers generated by the MRR systems can be used for an all optical generation of OFDM signals.

Acknowledgment

The gratitude also goes to the administration of Universiti Teknologi Malaysia (UTM) for providing research facilities and support.

References

[1] H. Bolcskei, D. Gesbert, and A. J. Paulraj, "On the capacity of OFDM-based spatial multiplexing systems," *IEEE Trans. Commun.*, vol. 50, no. 2, pp. 225–234, Feb. 2002.
[2] A. Attar, O. Holland, M. Nakhai, and A. Aghvami, "Interference-limited resource allocation for cognitive radio in orthogonal frequency-division multiplexing networks," *IET Commun.*, vol. 2, no. 6, pp. 806–814, Jul. 2008.
[3] H. L. Hung and Y. F. Huang, "Peak-to-average power ratio reduction in orthogonal frequency division multiplexing system using differential evolution-based partial transmit sequences scheme," *IET Commun.*, vol. 6, no. 11, pp. 1483–1408, Jul. 2012.
[4] K. N. Le and K. P. Dabke, "Channel capacity of OFDM systems employing diversity in fading environments," *Wireless Commun. Mobile Comput.*, vol. 12, no. 17, pp. 1493–1516, Dec. 2012.
[5] W. Shieh, X. Yi, Y. Ma, and Q. Yang, "Coherent optical OFDM: has its time come? [Invited]," *J. Opt. Netw.*, vol. 7, no. 3, pp. 234–255, Mar. 2008.
[6] N. Sreekanth and M. GiriPrasad, "BER analysis of mitigation of ICI through ICI self cancellation scheme in OFDM systems," *Int. J. Comput. Netw. Wireless Commun.*, vol. 2, no. 3, pp. 298–304, Jun. 2012.
[7] A. J. Lowery and J. Armstrong, "Orthogonal-frequency-division multiplexing for dispersion compensation of long-haul optical systems," *Opt. Exp.*, vol. 14, no. 6, pp. 2079–2084, Mar. 2006.
[8] W. Shieh, W. Chen, and R. Tucker, "Polarisation mode dispersion mitigation in coherent optical orthogonal frequency division multiplexed systems," *Electron. Lett.*, vol. 42, no. 17, pp. 996–997, Aug. 2006.
[9] Y. Benlachtar, P. M. Watts, R. Bouziane, P. Milder, D. Rangaraj, A. Cartolano, R. Koutsoyannis, J. C. Hoe, M. Püschel, M. Glick, and R. I. Killey, "Generation of optical OFDM signals using 21.4 GS/s real time digital signal processing," *Opt. Exp.*, vol. 17, no. 20, pp. 17 658–17 668, Sep. 2009.
[10] Q. Yang, S. Chen, Y. Ma, and W. Shieh, "Real-time reception of multi-gigabit coherent optical OFDM signals," *Opt. Exp.*, vol. 17, no. 10, pp. 7985–7992, May 2009.
[11] H. Chen, M. Chen, and S. Xie, "All-optical sampling orthogonal frequency-division multiplexing scheme for high-speed transmission system," *J. Lightwave Technol.*, vol. 27, no. 21, pp. 4848–4854, Nov. 2009.
[12] Z. Wang, K. S. Kravtsov, Y.-K. Huang, and P. R. Prucnal, "Optical FFT/IFFT circuit realization using arrayed waveguide gratings and the applications in all-optical OFDM system," *Opt. Exp.*, vol. 19, no. 5, pp. 4501–4512, Feb. 2011.
[13] I. S. Amiri, S. E. Alavi, and J. Ali, "High capacity soliton transmission for indoor and outdoor communications using integrated ring resonators," *Int. J. Commun. Syst.*, DOI: 10.1002/dac.2645, to be published.
[14] I. S. Amiri, A. Afroozeh, and M. Bahadoran, "Simulation and analysis of multisoliton generation using a PANDA ring resonator system," *Chin. Phys. Lett.*, vol. 28, no. 10, p. 104 205, Oct. 2011.
[15] M. Spyropoulou, N. Pleros, and A. Miliou, "SOA-MZI-based nonlinear optical signal processing: A frequency domain transfer function for wavelength conversion, clock recovery, and packet envelope detection," *IEEE J. Quantum Electron.*, vol. 47, no. 1, pp. 40–49, Jan. 2011.
[16] I. S. Amiri, R. Ahsan, A. Shahidinejad, J. Ali, and P. P. Yupapin, "Characterisation of bifurcation and chaos in silicon microring resonator," *IET Commun.*, vol. 6, no. 16, pp. 2671–2675, Nov. 2012.
[17] I. S. Amiri, A. Nikoukar, and J. Ali, "GHz frequency band soliton generation using integrated ring resonator for WiMAX optical communication," *Opt. Quantum Electron.*, DOI: 10.1007/s11082-013-9848-0, to be published.
[18] S. Lin and K. B. Crozier, "Planar silicon microrings as wavelength-multiplexed optical traps for storing and sensing particles," *Lab Chip*, vol. 11, no. 23, pp. 4047–4051, Dec. 2011.
[19] I. S. Amiri, S. E. Alavi, S. M. Idrus, A. Nikoukar, and J. Ali, "IEEE 802.15.3c WPAN standard using millimeter optical soliton pulse generated by a panda ring resonator," *IEEE Photon. J.*, vol. 5, no. 5, p. 7901912, Oct. 2013.

[20] I. S. Amiri and J. Ali, "Generating highly dark–bright solitons by Gaussian beam propagation in a PANDA ring resonator," *J. Comput. Theor. Nanosci.*, vol. 11, no. 4, 2014.
[21] I. S. Amiri and J. Ali, "Optical quantum generation and transmission of 57-61 GHz frequency band using an optical fiber optics," *J. Comput. Theor. Nanosci.*, vol. 11, no. 10, 2014.
[22] S. Kumar, R. Egorov, K. Croussore, M. Allen, M. Mitchell, and B. Basch, "Experimental study of intra-vs. inter-superchannel spectral equalization in flexible grid systems," presented at the Optical Fiber Communication Conference, Anaheim, CA, USA, 2013, Paper JW2A.05.
[23] C.-E. Chou, N.-H. Sun, and W.-F. Liu, "Gain flattening filter of an erbium-doped fiber amplifier based on etching long-period gratings technology," *Opt. Eng.*, vol. 43, no. 2, pp. 342–345, Feb. 2004.
[24] I. S. Amiri, K. Raman, A. Afroozeh, M. A. Jalil, I. N. Nawi, J. Ali, and P. P. Yupapin, "Generation of DSA for security application," *Proc. Eng.*, vol. 8, pp. 360–365, 2011.
[25] I. S. Amiri, A. Nikoukar, A. Shahidinejad, T. Anwar, and J. Ali, "Quantum transmission of optical tweezers via fiber optic using half-panda system," *Life Sci. J.*, vol. 10, no. 12s, pp. 391–400, Dec. 2013.
[26] I. S. Amiri, J. Ali, and P. P. Yupapin, "Enhancement of FSR and finesse using add/drop filter and PANDA ring resonator systems," *Int. J. Mod. Phys. B*, vol. 26, no. 4, pp. 1250034-1–1250034-13, Feb. 2012.
[27] I. S. Amiri and J. Ali, "Femtosecond optical quantum memory generation using optical bright soliton," *J. Comput. Theor. Nanosci.*, vol. 11, no. 6, 2014.
[28] I. S. Amiri, P. Naraei, and J. Ali, "Review and theory of optical soliton generation used to improve the security and high capacity of MRR and NRR passive systems," *J. Comput. Theor. Nanosci.*, vol. 11, no. 9, 2014.
[29] I. S. Amiri, F. J. Rahim, A. S. Arif, S. Ghorbani, P. Naraei, D. Forsyth, and J. Ali, "Single soliton bandwidth generation and manipulation by microring resonator," *Life Sci. J.*, vol. 10, no. 12s, pp. 904–910, Dec. 2013.
[30] I. S. Amiri, S. Soltanmohammadi, A. Shahidinejad, and J. Ali, "Optical quantum transmitter with finesse of 30 at 800-nm central wavelength using microring resonators," *Opt. Quantum Electron.*, vol. 45, no. 10, pp. 1095–1105, Oct. 2013.
[31] I. S. Amiri, A. Afroozeh, I. N. Nawi, M. A. Jalil, A. Mohamad, J. Ali, and P. P. Yupapin, "Dark soliton array for communication security," *Proc. Eng.*, vol. 8, pp. 417–422, 2011.
[32] I. S. Amiri and J. Ali, "Nano particle trapping by ultra-short tweezer and wells using MRR interferometer system for spectroscopy application," *Nanosci. Nanotechnol. Lett.*, vol. 5, no. 8, pp. 850–856, Aug. 2013.
[33] I. S. Amiri, A. Nikoukar, A. Shahidinejad, J. Ali, and P. Yupapin, "Generation of discrete frequency and wavelength for secured computer networks system using integrated ring resonators," in *Proc. ICCCE*, Kuala Lumpur, Malaysia, 2012, pp. 775–778.
[34] N. Suwanpayak, M. A. Jalil, C. Teeka, J. Ali, and P. P. Yupapin, "Optical vortices generated by a PANDA ring resonator for drug trapping and delivery applications," *Biomed. Opt. Exp.*, vol. 2, no. 1, pp. 159–168, Jan. 2011.
[35] I. S. Amiri, M. Ranjbar, A. Nikoukar, A. Shahidinejad, J. Ali, and P. Yupapin, "Multi optical soliton generated by PANDA ring resonator for secure network communication," in *Proc. ICCCE*, Kuala Lumpur, Malaysia, 2012, pp. 760–764.
[36] M. Jalil, A. Abdolkarim, T. Saktioto, C. Ong, and P. P. Yupapin, "Generation of THz frequency using PANDA ring resonator for THz imaging," *Int. J. Nanomed.*, vol. 7, pp. 773–779, Feb. 2012.
[37] K. Luangxaysana, S. Mitatha, M. Yoshida, N. Komine, and P. Yupapin, "High-capacity terahertz carrier generation using a modified add-drop filter for radio frequency identification," *Opt. Eng.*, vol. 51, no. 8, pp. 085006-1–085006-7, Aug. 2012.
[38] I. S. Amiri and J. Ali, "Picosecond soliton pulse generation using a PANDA system for solar cells fabrication," *J. Comput. Theor. Nanosci.*, vol. 11, no. 3, pp. 693–701, Mar. 2014.
[39] I. S. Amiri and J. Ali, "Data signal processing via a manchester coding-decoding method using chaotic signals generated by a PANDA ring resonator," *Chin. Opt. Lett.*, vol. 11, no. 4, p. 041901, Apr. 2013.
[40] S. E. Alavi, I. S. Amiri, S. M. Idrus, A. S. M. Supa'at, and J. Ali, "Chaotic signal generation and trapping using an optical transmission link," *Life Sci. J.*, vol. 10, no. 9s, pp. 186–192, Sep. 2013.
[41] S. E. Alavi, I. S. Amiri, S. M. Idrus, and J. Ali, "Optical wired/wireless communication using soliton optical tweezers," *Life Sci. J.*, vol. 10, no. 12s, pp. 179–187, Dec. 2013.
[42] P. Yupapin and W. Suwancharoen, "Chaotic signal generation and cancellation using a micro ring resonator incorporating an optical add/drop multiplexer," *Opt. Commun.*, vol. 280, no. 2, pp. 343–350, Dec. 2007.
[43] I. Sadegh Amiri, M. Nikmaram, A. Shahidinejad, and J. Ali, "Generation of potential wells used for quantum codes transmission via a TDMA network communication system," *Security Commun. Netw.*, vol. 6, no. 11, pp. 1301–1309, Nov. 2013.
[44] I. S. Amiri, M. H. Khanmirzaei, M. Kouhnavard, P. P. Yupapin, and J. Ali, "Quantum entanglement using multi dark soliton correlation for multivariable quantum router," in *Quantum Entanglement*, A. M. Moran, Ed. Commack, NY, USA: Nova, 2012, pp. 111–122.